

Simple Calculation of the Anisotropic Factor for Minimum Current Path in MgB_2 Material Using the Extrapolated Kramer Field as *priori* Parameter

(Pengiraan Ringkas Faktor Ketakisotropian Untuk Lintasan Arus Minimum dalam Bahan MgB_2 Menggunakan Medan Kramer Unjuran Sebagai Parameter *Priori*)

M.I. ADAM*, M. F.M. ARIS, S.K. CHEN & S.A. HALIM

ABSTRACT

The volume flux pinning force density of Mg_xB_2 ($x = 0.8, 1.0$ and 1.2) materials was calculated for grain boundary and point pinning potentials. Stoichiometric $Mg_{0.8}B_2$, MgB_2 , and $Mg_{1.2}B_2$ samples were prepared by the conventional solid state reaction method. Three pellets were annealed at temperature range of 650–800°C. Structural analysis revealed large values for FWHM at (hkl) (110)(°) which indicates distortion in the boron plane of these specimens. The a and c – axis lattice parameters showed respective contraction and elongation with the increase in processing temperature. The low crystallinity found in $Mg_{0.8}B_2$ and $Mg_{1.2}B_2$ specimens was concluded to be due to structural defects, which act as flux pinning centres. Experimental anisotropic factor and the minimum fraction for current path, obtained from the framework of current percolation theory were used to explain the strong field dependence of the critical current density, J_c in the specimens. The summit of the maximum pinning force density was shifted to lower magnetic field position with the increase of anisotropy. The scaling laws were employed in a Kramer–like field in order to identify the dominant pinning mechanism correspondence to the summit of maximum pinning. For MgB_2 specimens however, a renormalization field based on the current percolation exposition is considered for the identification of their dominant pinning since it is very difficult to account for the flat behaviour of the pinning force in the weakened current region of these specimens.

Keywords: Anisotropy; current percolation; grain boundary pinning

ABSTRAK

Ketumpatan daya pengepin isipadu fluks dalam bahan Mg_xB_2 ($x = 0.8, 1.0, 1.2$) dikira untuk keupayaan pengepinan titik dan sempadan butiran. Bahan berstoikiometri $Mg_{0.8}B_2$, MgB_2 , dan $Mg_{1.2}B_2$ disediakan melalui kaedah tindak balas keadaan pepejal. Tiga pelet disepuhlandap dalam julat suhu 650–800°C. Analisis struktur menzahirkan nilai 'FWHM' yang besar pada (hkl) (110)(°) yang menunjukkan herotan pada satah boron bahan tersebut. Pemalar kekisi paksi- a dan c menunjukkan pengecutan dan pemanjangan apabila suhu meningkat. Kerendahan ciri kehabluran dalam bahan $Mg_{0.8}B_2$ dan $Mg_{1.2}B_2$ adalah disebabkan oleh kecacatan struktur yang bertindak sebagai pusat pengepin fluks. Faktor ketakisotropian uji kaji dan pecahan minimum yang diperolehi daripada rangka kerja teori perkolasi laluan arus digunakan untuk menjelaskan kebergantungan yang kuat ketumpatan arus genting J_c dalam bahan. Ketumpatan daya pengepin maksimum tersesar ke kedudukan rendah dengan penambahan ketakisotropian. Hukum penskalan digunakan dalam medan bak-Kramer untuk mengenalpasti mekanisme pengepinan dominan yang sepadan dengan puncak maksimum pengepinan. Walau bagaimanapun, untuk bahan MgB_2 suatu medan ternormal berdasarkan kedudukan arus perkolasi diambil kira untuk penentuan pengepinan dominan kerana adalah agak sukar untuk menentukan sifat daya pengepinan yang mendatar dalam daerah arus yang lemah di dalam bahan.

Kata kunci: Anisotropi; arus perikolasi; pengepinan sempan butiran

INTRODUCTION

The huge scientific interests recently triggered by the property of superconductivity in polycrystalline MgB_2 is primarily due to low cost, relative structural simplicity and the apparent superiority of its critical current density J_c , compared to other well-known cuprates superconductors. It was soon pointed out to the similarity between MgB_2 and Nb_3Sn , a conventional low temperature superconductor in which the grain boundary is a major point for strong flux pinning (Larbalestier et al. 2001). J_c in MgB_2 is however

known to possess very strong magnetic field dependence and the J_c decreases exponentially at high fields and temperatures. Subsequently, a great amount of work is being done in order to improve the J_c in bulk, wires, and thin film forms of this compound and several processing techniques were yet adopted in this regard. Relatively low temperature sintering (Yamamoto et al. 2006), carbon and ferromagnetic oxide doping (Qu et al. 2009), grain size reduction (Mikheenko et al. 2007) and, neutron bombardment (Eisterer et al. 2007) techniques were

mostly directed towards slowing the field dependence of J_c , especially at 20–25K, the targeted operating temperature for large-scale applications.

On the other hand, the scaling laws previously used to explain many experimental findings of conventional superconductors were eventually validated for usage to studying the MgB_2 material due to its similarity in flux pinning aspects with the likes of Nb_3Sn alloy superconductor. The field dependence of J_c in MgB_2 is recently modeled (Eisterer et al. 2003) based on the anisotropic London theory and the percolation theory for the grains boundary pinning. The rather low upper critical field values deduced from the samples were found to strongly dictate the critical current density J_c . A scaling procedure is thus proposed for volume pinning identification in anisotropic MgB_2 . However, the proposed scaling procedure is found to account only for the anisotropic MgB_2 . We further modified the Kramer plot employing a specimen-specific scaling procedure in order to account for the small anisotropy and the relatively large continuous current path in $\text{Mg}_{0.8}\text{B}_2$ and $\text{Mg}_{1.2}\text{B}_2$ specimens. We also investigated the volume flux pinning property in non-stoichiometric Mg_xB_2 specimens. Deduced pinning characteristics were compared and related to anisotropy, and the minimum fraction for continuous current path was estimated from these specimens. Pinning parameters were calculated for the anisotropic irreversibility field H_{irr} and the upper critical field H_{c2} is thus found.

EXPERIMENTAL PROCEDURE

Polycrystalline specimens of Mg_xB_2 ($x = 0.8, 1.0, 1.2$) were prepared by reacting commercial Mg and B powders. Magnesium ($< 10 \mu\text{m}$) and amorphous boron were weighted accordingly and well mixed by grinding them in mortar by using a pestle. The mixture was then pressed into pellets of 12 mm diameter and 2 mm thickness by using a hydraulic press with the applied pressure of 0.4 GPa. The pellets were sealed into iron tubes for annealing in a tube furnace in high purity argon gas flow environment. Different set of specimens were prepared by annealing the pellets at temperatures of 650, 700, 750 and 800°C, respectively for 1 h. The heating and cooling rates used were 10°C/min. Commercial Quantum Design DC Magnetic Properties Measurement System (MPMS-XL) was used to obtain the superconducting transition temperature, T_c and magnetisation hysteresis loops. Magnetic J_c was estimated based on the critical state model.

RESULTS AND DISCUSSION

Table 1 shows the full width at half maximum, (FWHM) data collected from XRD results for (hkl) (110)(°) together with other physical parameters for all specimens studied. Large (FWHM) values for $\text{Mg}_{0.8}\text{B}_2$ and $\text{Mg}_{1.2}\text{B}_2$ specimens were compared to that of the stoichiometric MgB_2 . Large FWHM value indicates poor crystallinity in these specimens. Elongation in c – axis and contraction in a – axis parameters shown as a ratio c/a in Figure 1 is clear evidence of crystallinity deterioration above and below the Mg stoichiometric region of $x = 1.0$. Note that in the as – weighted Mg : B powders ratio of 0.8: 2, 1.0: 2, and 1.2: 2, it is very difficult to ascertain the exact amount of both Mg and B constituents in the final product. A small amount of MgO and MgB_4 secondary phases certainly form during reaction process at the expense of the as – weighted powders. Therefore, the compositional variation indicator, x for nominal Mg in the Mg_xB_2 specimens may only refers to initial weighting composition but not the final product.

The J_c versus the applied magnetic field up to 8T at 20K is shown in Figure 2 for specimens processed at 800°C. J_c values were calculated from the magnetization curves according to the derivations of the extended critical state model (Chen & Goldfarb 1989). We note that the observed decrease of J_c in $\text{Mg}_{0.8}\text{B}_2$ specimen at low fields is quite unusual and might be an artefact of the measurement (flux jumps, self-field, etc.). Higher values of J_c for both $\text{Mg}_{1.2}\text{B}_2$ and $\text{Mg}_{0.8}\text{B}_2$ specimens were seen at higher magnetic fields. The specimen MgB_2 however exhibits lower J_c value at 20 K at higher magnetic fields as compared to the other specimens. At nearly zero magnetic field, the measured J_c for $\text{Mg}_{1.2}\text{B}_2$ and MgB_2 specimens at 20K starts at $2.0 \times 10^5 \text{A cm}^{-2}$. A J_c value of $\sim 1.0 \times 10^5 \text{A cm}^{-2}$ was also observed in $\text{Mg}_{0.8}\text{B}_2$ specimen.

The scaling laws, (Eisterer et al. 2003, 2007, 2008; Kramer 1973, 1978), extensively used to approximate the volume pinning force density, $f_p(b)$ at specific temperature and magnetic field induction B can be written as

$$f_p \left(\frac{B}{B_{irr}} \right) = F_p \left(\frac{B}{B_{irr}} \right) \alpha \left(\frac{B}{B_{irr}} \right)^m \left(1 - \frac{B}{B_{irr}} \right)^n; \quad (1)$$

$$f_p(b) = F_p(b) \alpha (b)^m (1-b)^n$$

TABLE 1. Structural and superconducting parameters deduced from all specimens for the determination of flux pinning property

Specimen	(110)(°)				T_c (K)	B_{irr} (T)	B_{c2} (T)	B_{irr}/B_n (T)
	650°C	700°C	750°C	800				
$\text{Mg}_{0.8}\text{B}_2$	0.444	0.389	0.376	0.361	37.02	7.50	14.80	7.50/.....
MgB_2	0.408	0.385	0.348	0.340	38.07	3.80	14.6/29.2	4.20/8.40
$\text{Mg}_{1.2}\text{B}_2$	0.404	0.390	0.355	0.347	37.20	7.20	13.30	7.20/.....

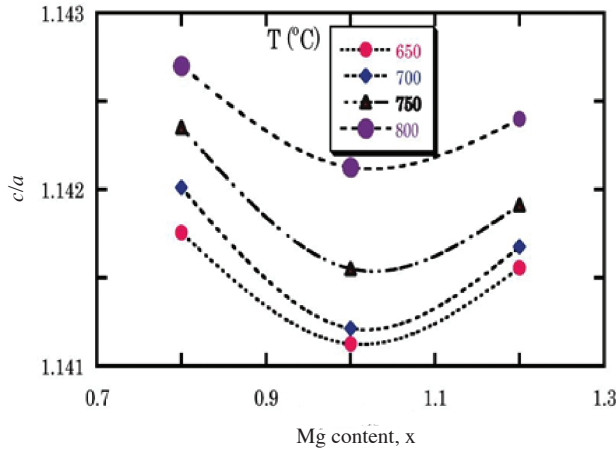


FIGURE 1. The ratio c/a of the lattice parameters as a function of Mg content x For $Mg_{0.8}B_2$, MgB_2 , and $Mg_{1.2}B_2$ pellets annealed in argon at different temperatures as shown in the legend. Discrete lines serve as guide to the eye

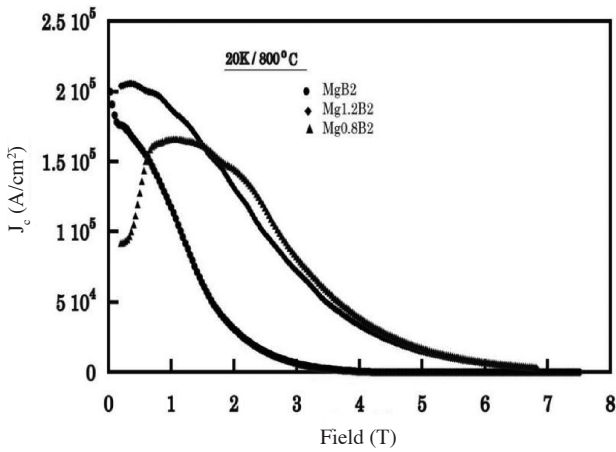


FIGURE 2. Critical current density (J_c) measured at 20K at varying field for $Mg_{0.8}B_2$, MgB_2 , and $Mg_{1.2}B_2$ pellets annealed in argon at 800°C

where $b = \frac{B}{B_{irr}} \approx \frac{B}{B_{c2}}$, $F_p = \frac{F_p}{F_{p,max}}$ with B , B_{irr} , B_{c2} denote the applied magnetic field, the irreversibility field and the upper critical field, respectively. F_p , $F_{p,max}$ are the global flux pinning force density and its maximum value. m and n are pinning parameters. For MgB_2 materials, B_{irr} was found to be much influenced by anisotropy, grain connectivity and the volume fraction of conducting grains. The later factor is restricted by the presence of voids and secondary phases. As a result, B_{irr} the field where J_c approaches zero, occurs at fields much below the upper critical field, B_{c2} . Hence, the strong field dependence of J_c in this class of materials necessitates the usage of different approach in order to account for B_{c2} to a certain degree of accuracy. One of the methods convincingly used for the estimation of B_{irr} is the Kramer plot for $J_c^{0.5} B^{0.25}$ vs. B , as shown in Figure 3. B_{irr} is extrapolated from the most linear part of $J_c^{0.5} B^{0.25}$ vs. B curve, measured at 20K for all specimens heat-treated at 800°C. The intersection of the extrapolated line with

the reduced field axis gives a rough estimation for the value of B_{irr} as indicated by the arrow head in the Figure. It is apparent that the J_c retains very small value at higher fields, (see Figures 2 to 5 for actual field and reduced field values). This feature is quite clear in MgB_2 specimen as its J_c started to approach zero at reduced field just above 0.52. As pointed out in reference (Eisterer 2008), extrapolation of the Kramer plot for the estimation of Kramer field and/or B_{irr} , as shown in Figure 3 for MgB_2 specimen does not seem to be directly relate to one of the relevant parameters, (B_{c2} , anisotropic factor, γ and the minimum fraction of superconducting grains for a continuous current path p_c) but a complicated function of these parameters.

Since the current flow in both $Mg_{1.2}B_2$ and $Mg_{0.8}B_2$ specimens show rather high values at considerably high fields, we shall first treat all the specimens in a modified Kramer plot, in order to account for the above-mentioned pinning force density parameters. A modified scaling procedure shall then be used to gauge the pinning property of MgB_2 specimen. Nevertheless, for MgB_2 specimen, J_c remains above zero in value to fields well above B_{irr} (i.e. $B_{irr}^{ab} > B_{irr}$) due to the availability of a small but finite current path in the superconducting grains. The current percolation model for anisotropic MgB_2 assumes that

$$J_c \propto \frac{[1 - B/B_{c2}(\theta)]^2}{\sqrt{B_{c2}(\theta)B}} \quad \text{for } B \leq B_{c2} \text{ and } J_c \perp B \quad (2)$$

Equation (2) strictly considers the weakening behaviour of J_c at higher magnetic fields and the rapid decrease of current at low fields observed in most MgB_2 samples. θ is the angle between boron layers in the grains, and field B is defined in the anisotropic Ginsburg – Landau equation, (Tilley 1965) where

$$B_{c2}(\theta) = B_{c2} / \sqrt{\gamma^2 \cos^2 \theta + \sin^2 \theta} \quad (3)$$

$\gamma = B_{c2||}/B_{c2\perp}$ represents the anisotropic factor of B_{c2} . Here, θ is the angle of orientation for the applied magnetic field with respect to the crystallographic c axis. However, the scaling laws for volume pinning force and the macroscopic irreversibility field for normalization were derived assuming that the intrinsic irreversibility field $B_{irr} = B_{c2}$;

Hence, the relation between these fields in anisotropic medium can be given by

$$B_{irr} = B_{c2} / \sqrt{(\gamma^2 - 1)p_c^2 + 1} \quad (4)$$

where p_c is the minimum fraction for continuous current path within the superconducting grains. Note that further modification to equation (4) is possible if the extrapolated B_{irr} is much smaller than B_{c2} , considering the effect of both γ and p_c at specific temperature. This approach is much suited for anisotropic materials such as MgB_2 , as demonstrated in Figure 4 for all specimens studied.

Extrapolated Kramer fields were shown in Figure 3 for all specimens. These fields were reproduced in a

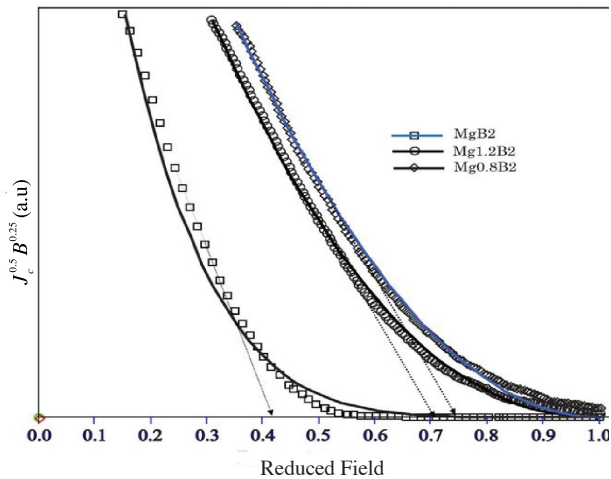


FIGURE 3. Experimental Kramer plot for MgB_2 specimens. Kramer fields are directly extrapolated to a reduced field value without considering the influence of anisotropy and current percolation path

theoretically modified Kramer plot as shown in Figure 4 employing a specimen-specific scaling procedure for the determination of parameters affecting the volume pinning force density. The plot is shown in a plane which contains data for three other polycrystalline MgB_2 of the same minimum current path efficiency, $p_c = 0.25$ but different anisotropy. As can be seen from Equation (4) and Figure 4, γ and p_c parameters have greater influence on the overall pinning force density of the specimens. Anisotropic factor of $\text{Mg}_{0.8}\text{B}_2$ and $\text{Mg}_{1.2}\text{B}_2$ specimens are similar to that of anisotropic materials with $\gamma = 2.0$. p_c for these specimens are 0.55 and 0.46, respectively. It is reported that thermal fluctuations and material inhomogeneity increase the value of p_c , (Eisterer et al. 2003). Hence, the relatively large value of p_c can be related to the preparation history

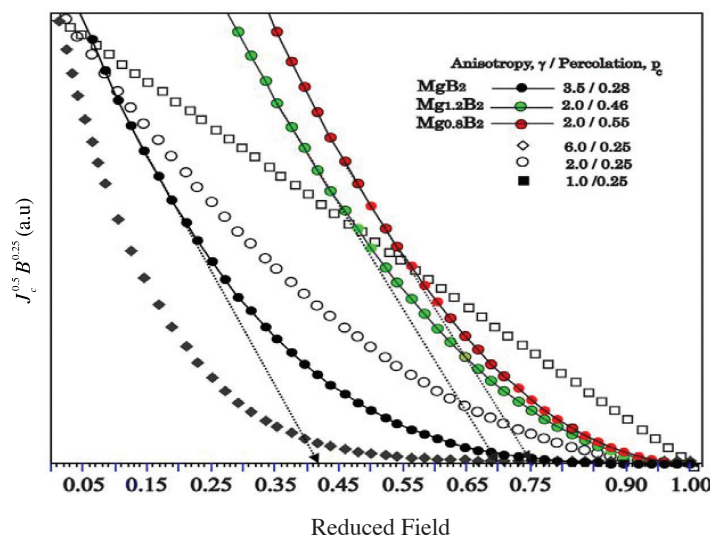


FIGURE 4. Reproduction of the Kramer plot for the data shown in Figure 2 with different anisotropies and current percolation path values. Data were plotted in an Eisterer – like plane to indicate a possible limit for anisotropy in MgB_2 materials

of these specimens. Experimental data of the normalized pinning force density for all specimens is plotted against the reduced magnetic field in Figure 5. Theoretical curves based on equation (1) for isotropic and anisotropic grain boundary pinning were also shown, (dashed–line curves). It is obvious that the summit of the isotropic curve, (dash-dotted curve) is proportional to the reduced field value of 0.2. Summits of the experimental data are however specimen dependent. Their respective reduced field values are 0.13, 0.23, and 0.28 for MgB_2 , $\text{Mg}_{1.2}\text{B}_2$, and $\text{Mg}_{0.8}\text{B}_2$, respectively. p_c can also be calculated as the ratio of secondary phase and/or the statistical average of the grains size from electrical connectivity data (Matsushita et al. 2008; Yamamoto et al. 2007). Theoretical determination of finite lattice site percolation in higher dimensions is also used for the estimation of p_c in various superconductors (Stauffer & Aharony 1998). p_c of 0.25 with a corresponding γ of 1.00 is reported in reference (Eisterer 2008) for MgB_2 sample in the isotropic case, (refers to peak position at 0.1 reduced field). The same values were reproduced in the calculations of the theoretical curves shown in Figures 4 and 5. The anisotropic curve, (dashed–line curve in Figure 5) gives γ & p_c of 2.0 & 0.25, respectively.

Based on the analysis demonstrated above for the estimation of various parameters, we calculated the pinning force density, $f_p = J_c \times B$ for all specimens at $800^\circ\text{C}/20\text{K}$. The results are shown in Figure 5. Satisfactory agreement is obtained for each experiment with different γ and p_c values, as shown in the legend of Figure 4. The specimen dependent γ and p_c for MgB_2 specimen are 3.5 and 0.28. These values are similar to those reported in reference (Eisterer et al. 2003). For $\text{Mg}_{0.8}\text{B}_2$ and $\text{Mg}_{1.2}\text{B}_2$ specimens however, their reduced field values of 0.28 and 0.23 were found to be very close to the un – rescaled values reported for MgB_2 material with anisotropic factor, $\gamma = 4.0$ (see Eisterer 2008). Hence, these parameters were

used to calculate B_{c2} using equation (4). The $Mg_{0.8}B_2$ and $Mg_{1.2}B_2$ specimens were found to contain small anisotropy and a relatively large minimum current path as shown in Figures 4 and 5. A smaller anisotropic factor resulted in the occurrence of B_{irr} at fields about 70% and 75% near the full range of the reduced field. This favourable effect is oppositely encountered by a large percolative current path due to specimen inhomogeneity. The actual effect of p_c in these specimens therefore, is to delay the occurrence of the maximum pinning force density to 28% and 23% of reduced field range.

From the viewpoint of materials structure, defects, secondary phases and porosity are very important factors for clarifying the pinning mechanism in the $Mg_{0.8}B_2$ and $Mg_{1.2}B_2$ specimens. The presence of unreacted amorphous boron in a boron-deficient specimen is found to act as additional pinning centres and further enhanced J_c (Vilas et al. 2006). The critical temperature T_c , measured as the onset of diamagnetism from ac susceptibility curves, listed in Table 1 for these specimens, is also lower than that for MgB_2 . Furthermore, representation of the normalized pinning force versus the reduced field for $Mg_{0.8}B_2$ and $Mg_{1.2}B_2$ specimens is seen to satisfy both the Kramer and the modified Kramer plots, (see Figures 4 and 5). Hence, the extrapolated field (B_{irr}) depicted in these figures is used for the calculation of the upper critical field, B_{c2} using Equation (4). Reasonable value for B_{c2} is found and listed in Table 1 for each specimen. Values of parameter m and n from equation (1) specify the dominant pinning force density in Nb_3Sn and MgB_2 materials (Sangjun & Keeman 2006; Cheng et al. 2007).

Parameter m ranges from 0.0 to 1.5 while parameter n ranges from 1.0 to 2.0 in value. The corresponding dominant pinning force density at these ranges includes normal core, surface, volume, point, and matrix pinning force densities. Theoretical curve, (dash-dotted curve) shown in Figure 5 describes the domination of normal core or surface pinning in an isotropic material with $m = 0.5$ and $n = 2.0$. The reduced isotropic peak field value in this case is 0.2. Grain boundary pinning force density dominates the pinning behaviour of anisotropic MgB_2 and results in reduced anisotropic peak field value of 0.10, (dashed-line curve in Figure 5) for similar m and n parameters. Pinning parameters for the data shown in Figures 5 identically fall in the range of m and n with the anisotropic grain boundary and point pinning force densities dominating the MgB_2 specimen, as deduced from peak position of the reduced magnetic field.

Figure 6 shows the experimental data for three MgB_2 specimens heat-treated at different temperatures. A field B_n , defined as the field at which the normalized pinning force density reach it's 50% value at fields above the peak field is used for renormalization. A scaling curve with $\gamma = 3.5$ and $p_c = 0.28$ is fitted to the data. The normalized pinning force peak position for all specimens shifted from 0.13 for B/B_{irr} to 0.49 for B/B_n . The expected pinning force density acting on the specimens current paths is seen to be point pinning since both γ and p_c fall at the dirty limit of these materials. However, the scaling curve shown in Figure 6 indicates no change in γ value due to renormalization by B/B_n . Note that the percolation path may be stretched twice a distance by the normalized pinning force.

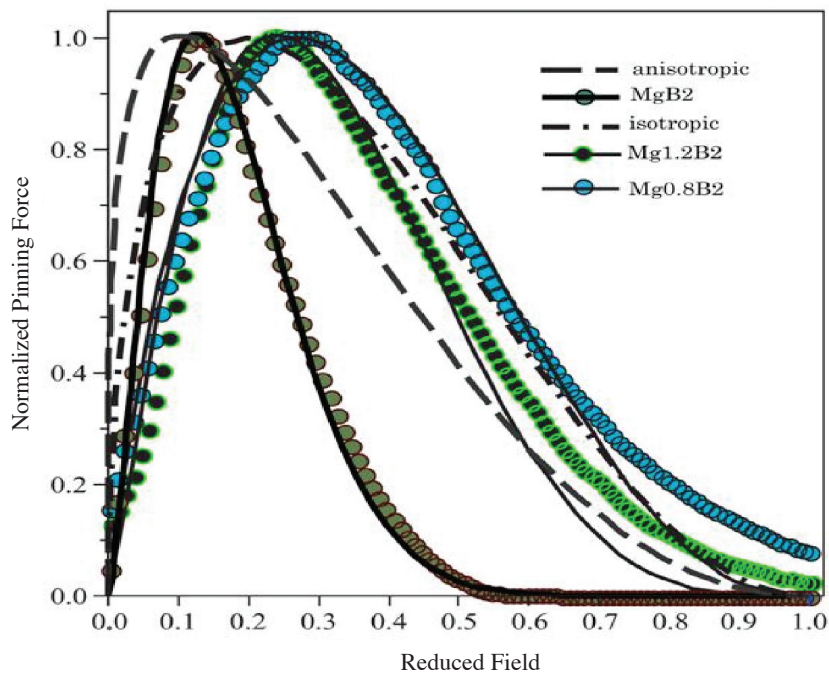


FIGURE 5. Normalized volume pinning force versus reduced field for the data shown in Figure 1. A standard curves for the global pinning force is also shown for comparison

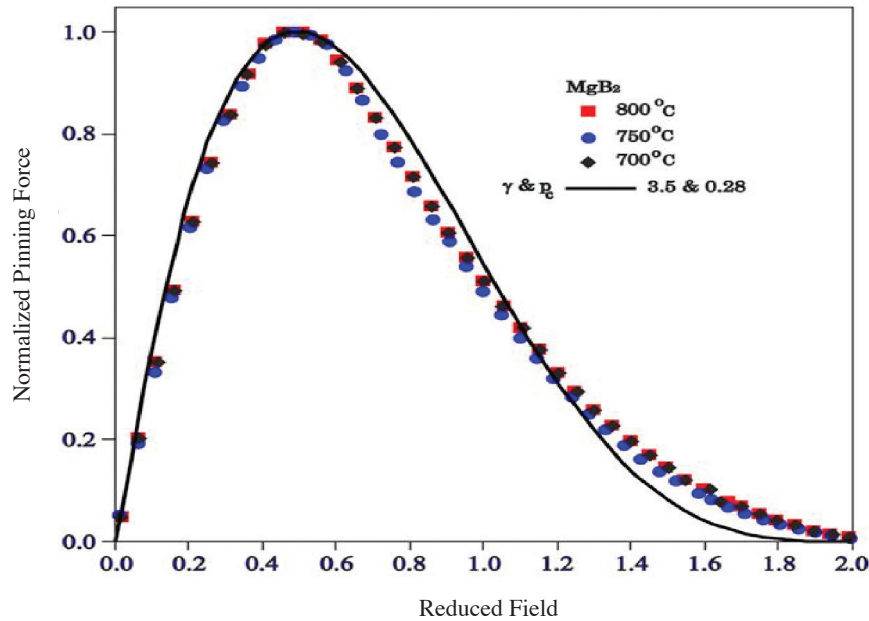


FIGURE 6. Field dependence of the volume pinning force for three nominal MgB_2 Specimens annealed at the temperatures given in the legend. Experimental data were scaled to B/B_n with the same γ and p_c factors

CONCLUSIONS

The volume flux pinning force density in $\text{Mg}_{1.2}\text{B}_2$, MgB_2 and $\text{Mg}_{0.8}\text{B}_2$ specimens were investigated. Defects and material inhomogeneity resulted in relatively large value of current percolation paths in the specimens. Structural analysis revealed large values for FWHM at (hkl) (110) ($^\circ$) which indicates distortion in the boron plane of these specimens. The a and c -axis constants showed respective contraction and elongation with the increase in processing temperature. Low crystallinity in $\text{Mg}_{0.8}$ and $\text{Mg}_{1.2}\text{B}$ specimens is concluded to be due to structural defects, which act as a flux pinning centres. This inferior structure is however found to enhance J_c and other pinning parameters at higher magnetic fields. Calculated anisotropic factor and the effective volume fraction of the superconducting current path for the specimens resulted in reasonable values for the estimated anisotropic irreversibility and upper critical fields.

ACKNOWLEDGEMENTS

The authors gratefully acknowledge financial support from the Research University Grant, (RU, Vote: 91147) and the Scientific Advancement Grant Allocation, (SAGA, Vote: 5486510). One of the authors (MIA) appreciates assistance received from the Department of Physics, University of Malaya.

REFERENCES

Chen, D.X. & Goldfarb, R.B., 1989. Kim model for magnetization of type – II Superconductors. *Journal of Applied Physics* 66: 2489-2500.

- Chen, S.K., Serquis, A., Serrano, G., Yates, K.A., Blamire, M.G., Guthrie, D., Cooper, J., Wang, H., Margadonna, S.M. & MacManus – Driscoll, J.L. 2008. Structural and superconducting property variations with nominal Mg non-stoichiometry in Mg_xB_2 and its enhancement of upper critical field. *Advanced Functional Materials* 18: 113-20.
- Cheng, C.H., Yang, Y., Munroe, P. & Zhao, Y. 2007. Comparison between Nano-diamond and carbon nanotube doping effects on critical current density and flux pinning in MgB_2 . *Superconductor Science & Technology* 20: 296-301.
- Eisterer, M., 2008. Calculation of the volume pinning force in MgB_2 superconductors. *Physical Review B* 77: 144524-1-5.
- Eisterer, M., Robert, S.K., Webber H.W., Sumption, M.D. & Bhatia, M. 2007. Neutron irradiation of SiC doped magnesium rich MgB_2 wires. *IEEE Transactions in Applied Superconductivity* 17: 2814-17.
- Eisterer, M., Zehetmayer, M. & Weber, H.W., 2003. Current percolation and anisotropy in polycrystalline MgB_2 . *Physical Review Letters* 90: 247002-1-4.
- Kramer, E.J. 1973. Scaling laws for flux pinning in hard superconductors. *Journal of Applied Physics*. 44: 1360 -70.
- Kramer, E.J. 1978. Fundamental fluxoid-defect interactions in irradiate superconductors. *Journal of Nuclear Materials* 72: 5-33.
- Larbalestier, D.C., Rikel, M.O., Cooley, L.D., Polyanskii, A.A., Jiang, J.Y., Patniak, S., Cai, X.Y., Feldmann, D.M., Gurevich, A., Squitieri, A.A., Naus, M.T., Eom, C.B. & Hellstrom, E.E. 2001. Strongly linked current flow in polycrystalline forms of the superconductor MgB_2 . *Nature* 410: 186-89.
- Matsushita, T., Kiuchi, M., Yamamoto, A., Shimoyama, J. & Kishio, K. 2008. Critical current density and flux pinning in superconducting MgB_2 . *Physica C* 568: 1833-35.
- Mikheenko, P., Martinez, E., Bevan, A., Abell, J.S. & MacManus – Driscoll, J.L., 2007. Grain boundaries and pinning in bulk MgB_2 . *Superconductor Science & Technology* 20: S264-70.

- Oh, Sangjun. & Kim, Keeman. 2006. A Consistent description of scaling laws for flux pinning in Nb_3Sn strands based on the Kramer Model. *IEEE Transactions in Applied Superconductivity* 16: 1216-19.
- Pol, Vilas Ganpat., Pol, Swati Vilas., Felner, Israel & Gednaken, Aharon. 2006. Critical current density in the MgB_2 nanoparticles prepared under autogenic pressure at elevated temperature. *Chemistry & Physics Letters* 433: 115-19.
- Qu, B., Sun, X.D., Li, J.G., Xiu, Z.M., Liu, S.H. & Hue, C.P. 2009. Significant improvement of critical current density in MgB_2 doped with ferromagnetic Fe_3O_4 nanoparticles. *Superconductor Science & Technology* 22: 015-027.
- Stauffer, D. & Aharony, A. 1998. *Introduction to Percolation Theory*. Taylor & Francis PA 19106.
- Tilley, D.R. 1965. The Ginsburg – Landau equations for anisotropic alloys. *Proceedings of the Royal Physical Society* 86: 289-95.
- Yamamoto, A., Shimomya, J., Kishio, K. & Matsushta, T. 2007. Limiting factors of normal – state conductivity in superconducting MgB_2 : an application of mean – field theory for a site percolation problem. *Superconductor Science & Technology* 20: 658-66.
- Yamamoto, A., Shimoyama, J., Ueda, S., Katsura, Y., Iwayama, I., Horii, S. & Kishio, K. 2006. Crystallinity and flux pinning properties of MgB_2 bulks. *Physica C* 445-448: 806-10.
- M.I. Adam*
Dept of Physics
Faculty of Science
University of Malaya
50603 Kuala Lumpur
Malaysia
- M.F.M. Aris & S.K. Chen
Dept of Physics
Faculty of Science
Universiti Putra Malaysia
43400 UPM, Serdang, Selangor
Malaysia
- S.A. Halim
Institute For Mathematical Research (INSPEM)
Universiti Putra Malaysia
43400 UPM, Serdang, Selangor
Malaysia
- *Corresponding author; email: miadam@um.edu.my
- Received: 24 March 2010
Accepted: 17 January 2011